arXiv:1402.5879v1 [cond-mat.mes-hall] 24 Feb 2014

Electron coupling and density of states in rotated bilayer graphene

Omid Faizy Namarvar,[1,2,*] Guy Trambly de Laissardière,[3,†] and Didier Mayou[1,‡]

[1] *Université Grenoble Alpes, Institut NEEL, F-38042 Grenoble, France and CNRS, Institut NEEL, F-38042 Grenoble, France*

[2] *Centro S3, CNR - Istituto Nanoscienze, I-41125 Modena, Italy*

[3] *Laboratoire de Physique theorique et Modelisation, CNRS and Universite de Cergy-Pontoise, 95302 Cergy-Pontoise, France*

(Dated: February 25, 2014)

We study electronic structure of rotated bilayer graphene by using of tight-binding method and Green's functions techniques . A perturbative approach which is valid for not too small angles ($\theta \geq 3^\circ$) and states close to Dirac energy is developed. We calculate the self-energy of states of the upper plane due to their coupling with states of the lower plane . We discuss consequences for velocity renormalization and for electron-lifetime due to disorder in one plane. We also calculate and discuss the spatial modulations of density of states. We compare our analytical results to fully numerical calculations, showing good agreement between the two approaches.

PACS numbers: 73.22.Pr; 73.21.Ac

I. INTRODUCTION

Stacking several layers of Graphene on top of each other, may affect the original electronic structure. Indeed AB or Bernal stacking (as shown previously) destroys the linear dispersion and changes chirality properties even in a bilayer[1–6] Interaction between layers is then an important question. Yet as we will show in the following it does not systematically destroy interesting properties but on the contrary it can lead to the emergence of very peculiar and new behaviors.

Graphene can be formed in multilayers on SiC[4–12] but also on metal surfaces such as Ni[13] and in exfoliated flakes[14]) where interactions between successive layers play a crucial role. While on the Si face of SiC, multilayers have an AB stacking and do not show graphene properties[3–6] , on the C-face, multilayers have been shown to present graphene like properties even when they involve a large number of C planes. ARPES[9–12] , STM[15] , transport[16] and optical transitions[17] indeed show properties characteristic of a linear graphene like dispersion.

These multilayers are rotated with respect to each other and the rotations show up as Moiré patterns on STM images[10,18]. The Moiré effect is a well known phenomenon which occurs when repetitive structures (such as screens, grids or gratings) are superposed or viewed against each other. It consists of a new pattern of alternating dark and bright areas which is clearly observed at the superposition, although it does not appear in any of the original structures[?] . Moiré patterns are common in everyday life and often occur when two lattices overlap one another.

This apparent paradox of thick multilayers exhibiting graphene properties was partially solved recently when different theoretical approaches[10,19–26] showed that rotated multilayers are decoupled, at least for large rotation angles.

Going further, theory predicts the existence of three domains: for large rotation angles ($\theta > 20^\circ$) the layers are decoupled and behave as a collection of isolated graphene layers. For intermediate angles $3^\circ < \theta < 20^\circ$ the dispersion remains linear but the velocity is renormalized. What happens at the smallest values of θ is even more puzzling. As already shown by different theoretical groups, for the lowest θ, flat bands appear and result in electronic localization : states of similar energies, belonging to the Dirac cones of the two layers interact, a gap opens at the intersection, associated with saddle points. As the angle decreases, the saddle points come closer to the Dirac point and the renormalization of the velocity increases[19] .

Landau Level (LL) Scanning Tunneling Spectroscopy (STS) gave results in close agreement with theory. The three regimes where observed for CVD graphene grown on Ni: decoupling at large angle, renormalization and van Hove singularities for smaller angles. The singularities appear as peaks on both sides of E_D in STS experiments[13]. On the other hand, if decoupling is indeed observed for multilayers on C face of SiC (ARPES) velocity renormalization has never been shown for this system[11,12] . The origin of the different behavior between two so similar systems (both are rotated multi- layer graphene) and a possible discrepancy with theory is still subject to intense debate.

In this paper we develop a perturbative theory which gives us deeper insight in the regime $3^\circ < \theta < 20^\circ$ (intermediate angles). We recover known results for the velocity renormalization with a better justification for tight-binding model. We analyze also the effect of disorder in one plane on the lifetime of the other plane. We analyze also the spatial modulation of the DOS and demonstrate an increase of the DOS in AA region of the Moiré. This is a precursor of the localization in the AA region for very low angles less than 3°. This localization has already been observed in some systems and is predicted numerically.

II. TIGHT-BINDING MODEL AND HAMILTONIAN

In the tight-binding scheme only p_z orbitals are taken into account since we are interested in electronic states close to the

Fermi level. Since the planes are rotated, neighbors are not on top of each other (as is the case in the Bernal AB stacking). Interlayer interactions are then not restricted to $pp\sigma$ terms but some $pp\pi$ terms have also to be introduced[26].

The first thing is to compete the coupling between two states of two planes. Let us consider normalized Bloch states made of atomic orbitals A or B in plane α. One has

$$|\vec{K}_A\rangle_\alpha = \frac{1}{\sqrt{N}}\sum_{\vec{R}} e^{i\vec{K}\cdot\vec{R}_A}|A,R\rangle_\alpha \tag{1}$$

$$|\vec{K}_B\rangle_\alpha = \frac{1}{\sqrt{N}}\sum_{\vec{R}} e^{i\vec{K}\cdot\vec{R}_B}|B,R\rangle_\alpha \tag{2}$$

Where N is the number of unit cells of the crystal and the summation is perfumed on all cells of crystal. $\vec{R}$ is the position of A atom of the cell. In the following A or B are indicated by ε according to the following convention

$$\varepsilon = \begin{cases} +1 & \text{for A-atom} \\ -1 & \text{for B-atom} \end{cases} \tag{3}$$

$$\alpha = \begin{cases} +1 & \text{upper plane} \\ -1 & \text{lower plane} \end{cases} \tag{4}$$

We want to compute the matrix element of the Hamiltonian between two normalized Bloch states $|\varepsilon\vec{k}\rangle_+$ and $|\varepsilon'\vec{k'}\rangle_-$:

$$H_c(\varepsilon,\varepsilon';\vec{k},\vec{k'}) = \langle\vec{k'}\varepsilon'|H_c|\varepsilon\vec{k}\rangle = H_c(\vec{k'}\varepsilon';\vec{k}\varepsilon) \tag{5}$$

Because H_c is Hermitian, then we have:

$${}_+\langle\vec{k'}\varepsilon'|H_c|\varepsilon\vec{k}\rangle_- = \left({}_-\langle\varepsilon\vec{k}|H_c|\vec{k'}\varepsilon'\rangle_+\right)^* \tag{6}$$

$$H_c(\varepsilon,\varepsilon';\vec{k},\vec{k'}) = \sum_{\vec{R},\vec{R'}} e^{i(\vec{K}\cdot\vec{R}-\vec{K'}\cdot\vec{R'})}{}_-\langle\vec{R'}\varepsilon'|H_c|\varepsilon\vec{R}\rangle_+ \tag{7}$$

We have:

$$\begin{cases} \vec{r}_{\varepsilon\vec{R}}(\text{position in upper layer}) = \vec{R} & \text{if } \varepsilon = +1 \\ \vec{r}_{\varepsilon\vec{R}} = \vec{R}+\vec{u} & \text{if } \varepsilon = -1 \\ \vec{r'}_{\varepsilon'\vec{R'}}(\text{position in down layer}) = \vec{R'} & \text{if } \varepsilon' = +1 \\ \vec{r'}_{\varepsilon'\vec{R'}} = \vec{R'}+\vec{u'} & \text{if } \varepsilon' = -1 \end{cases} \tag{8}$$

Then

$${}_-\langle\vec{R'}\varepsilon'|H_c|\varepsilon\vec{R}\rangle_+ = H_c(|\vec{r}_{\varepsilon\vec{R}} - \vec{r'}_{\varepsilon'\vec{R'}}|) \tag{9}$$

where $\vec{u}$ and $\vec{u'}$ are vectors connecting the two atoms in the unit cells, i.e. A and B atoms in upper and A' and B' atoms in down layers respectively.

From Fourier transformation we write:

$$H_c(\vec{r}) = \int \widetilde{H}_c(\vec{k})\, e^{i\vec{k}\cdot\vec{r}}\, d^2\vec{k} \tag{10}$$

$$\widetilde{H}_c(\vec{k}) = \frac{1}{(2\pi)^2}\int H_c(\vec{r})\, e^{-i\vec{k}\cdot\vec{r}}\, d^2\vec{r} \tag{11}$$

Writing

$$H_c|\varepsilon\vec{k}\rangle_+ = \sum_i t(\varepsilon_i\vec{k}_i,\varepsilon\vec{k})\,|\varepsilon_i\vec{k}_i\rangle_- \tag{12}$$

Where $t(\varepsilon_i\vec{k}_i,\varepsilon\vec{k}) \equiv t_i$ is the transfer matrix element. We find selection rules such that

$$\vec{k}+\vec{K}_r = \vec{k'}+\vec{K'}_r \tag{13}$$

Which means that coupling Hamiltonian H_c couples the upper state $|\varepsilon\vec{k}\rangle_+$ to lower state $|\varepsilon\vec{k}\rangle_-$

Finally for $\vec{k}_i = \vec{k}+\vec{K}_r = \vec{k'}(mod\ \vec{K}'_r)$ we derive formula for coupling matrix after some calculations (Appendix B) we switch to the following expression of the Hamiltonian: Where $\vec{K}_r$ and $\vec{K}'_r$ are vectors of reciprocal lattices.

$$t_i(\vec{k}+\vec{K}_r) = \frac{4\pi^2}{S}\widetilde{H}_c(\vec{k}+\vec{K}_r)\, e^{i\,(\vec{k}+\vec{K}_r)\cdot(\varepsilon'\vec{u'}-\varepsilon\vec{u}+\vec{\Delta})} \tag{14}$$

Where S is area of unit cell, $\vec{\Delta}$ is translation between the two layers. However this translation of the two layers just translate the overall Moiré pattern and can be set to zero without loss of generality.

By symmetry of interaction between two orbitals, coupling depends only on the modulus of $\vec{k}+\vec{K}_r$ i.e $\widetilde{H}_c(\vec{k}+\vec{K}_r) \approx \widetilde{H}_c(|\vec{K}_d+\vec{K}_r|)$. The modulus of t_i is represented in Fig.1.

From Fig (2.9) one sees that the most important value of $|t_i|$ is one corresponding to the smallest possible value of $\vec{k}+\vec{K}_r$. By careful examination it can be shown that for electronic states close to the Dirac point this minimum corresponds to the modulus of wave-vector in Dirac point ($|\vec{K}_d| \approx 1.72$). From figure(coupling) it is easy to compute coupling value close Dirac is around 0.12eV. All the other contributions are much smaller and will be neglected here.

Selecting only this contribution means that $\vec{K}_r$ is such that $\vec{k}+\vec{K}_r$ belongs to one of three equivalent valleys. Therefore a set of two Bloch states with a given wave vector (equations 1 and 2) in one plane will be coupled to three sets of of two Bloch states in other plane corresponding to three different wave vectors. This simplifies much the structure of Hamiltonian and the analytical calculations presented here.

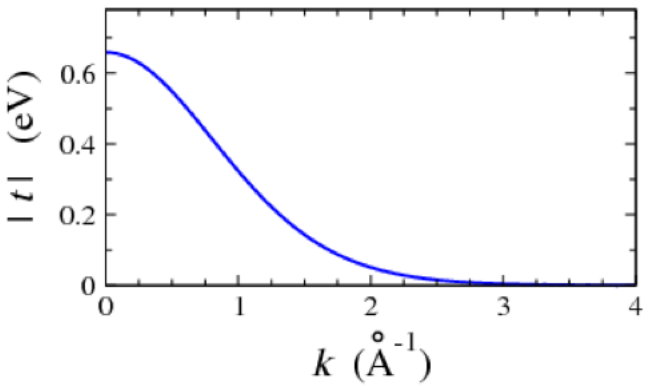

FIG. 1: Modulus of the inter-layer coupling in versus modulus of the wave-vector

III. VELOCITY RENORMALIZATION AND ELECTRON LIFE TIME

We are interested in the self-energy of coupling of states in upper plane due to the coupling with states of lower plane. Indeed the real-part of self-energy $\Re\sigma(z)$ is associated to modification of dispersion relation and will allow us to discuss velocity renormalization. The imaginary part of self-energy is associated to the electron lifetime. It will allow us to discuss lifetime of the electron in one plane when there is disorder in other plane.

Using matrix notations defined in Appendix B we have:

$$\widetilde{\Sigma}_0(z) = \sum_{\vec{K}_r} T_+(\vec{K}_r)\, \mathscr{G}_0^-\,(\vec{K}_d + \vec{K}_r)\, T_-(\vec{K}_r) \tag{15}$$

where $\vec{K}_r$ is the vector of reciprocal lattice which has three values as explanined above.

T describes the coupling between two plane and Green operator at wave vector $\theta\,\vec{\zeta}\times\vec{K}_\mu$ is

$$\mathscr{G}_0^-\,(z, \theta\,\vec{\zeta}\times\vec{K}_\mu) = \frac{1}{z - H_-(\theta\,\vec{\zeta}\times\vec{K}_\mu)} \tag{16}$$

where $\vec{K}_\mu$ counts three Dirac points.
and for the Hamiltonian:

$$H_-(\theta\,\vec{\zeta}\times\vec{K}_\mu) = \begin{pmatrix} -\gamma_1\, g(\theta\,\vec{\zeta}\times\vec{K}_\mu) + \Delta & -\gamma_0 f\,(\theta\,\vec{\zeta}\times\vec{K}_\mu) \\ -\gamma_0 f^*\,(\theta\,\vec{\zeta}\times\vec{K}_\mu) & -\gamma_1\, g(\theta\,\vec{\zeta}\times\vec{K}_\mu) + \Delta \end{pmatrix} \tag{17}$$

Where Δ is potential difference between two layers (plane(+) is in potential 0 and plane(-) is in potential Δ), $g = (|f|^2 - 3)$ is effect of next-nearest neighbor hoping of one plane[30] $\gamma_1 \approx 0.1$eV and:

$$f\,(\theta\,\vec{\zeta}\times\vec{K}_\mu) = |f\,(\theta\,\vec{\zeta}\times\vec{K}_\mu)|\; e^{i(\theta_\mu + \frac{\pi}{2}\varepsilon_\theta)}\; e^{i\alpha_-(\theta)} \tag{18}$$

where: $\varepsilon_\theta = \mathrm{sgn}(\theta)$, $\alpha_-(\theta) = \frac{2\pi\theta}{\sqrt{3}}$, is the next-nearest neighbor hoping and

$$|f\,(\theta\,\vec{\zeta}\times\vec{K}_\mu)| = \left|\gamma_0 e^{i\frac{2\pi}{\sqrt{3}}\theta}\left(1 - e^{-i\frac{2\pi}{\sqrt{3}}\theta}\right)\right| = 2\sin\frac{\pi\theta}{\sqrt{3}} \tag{19}$$

Note that this matrix is evaluated at $\theta\,\vec{\zeta}\times\vec{K}_\mu$. Indeed for $\vec{k}$ sufficiently close to Dirac point $\vec{k}$,

because $\hbar v(|\vec{k} - \vec{K}_d|) \ll \gamma_0 |f\,(\theta\,\vec{\zeta}\times\vec{K}_\mu)|$ and we can neglect the dependence on the $\vec{k}$ in H_-, $\mathscr{G}_-$ and $\widetilde{\Sigma}(z)$

So now after complex calculations (Appendix B) we can write a perfect relation for self-energy:

$$\widetilde{\Sigma}_0(z) = \sigma(z)\,\mathbf{I} \tag{20}$$

with $\mathbf{I}$ is identity matrix and

$$\begin{aligned} \sigma(z) &= \frac{6t^2}{\left[z - \gamma_1 g_(\theta)\right]^2 - \gamma_0^2 |f(\theta)|^2} \\ &\times \left[z - \Delta - \gamma_1 g_(\theta) - 2\gamma_0 \sin(\frac{\pi\theta}{\sqrt{3}})\sin(\frac{2\pi\theta}{\sqrt{3}})\right] \end{aligned} \tag{21}$$

Let us recall that the perturbation theory is valid for

$$z, t, \Delta \ll \gamma_0 f(\theta) \tag{22}$$

As shown below the important quantities are $\sigma(z)$ and its derivative $\sigma'(z)$. For both quantities we can neglect z in denominator. For simplicity we also neglect $g(\theta)$ and assimilate $|f(\theta)|$ and keep linear relation of $\sin\theta = \theta$:

$$\sigma(z) \approx \frac{-6t^2}{\gamma_0^2 \frac{4\pi^2}{3}\theta^2}\left[z - \Delta - \gamma_0^2 \frac{4\pi^2}{3}\theta^2\right] \tag{23}$$

A. Velocity renormalization

Using equation 19 we have every thing in hand to calculate the Green's function term in states $\vec{k}$ of the upper plane

$$\mathscr{G}_0^+ = \frac{1}{z - H_+(\vec{k}) - \tilde{\Sigma}_0(z)} = \begin{pmatrix} z - \sigma(z) & -\hbar v|\vec{k}|e^{i\theta(\vec{k})} \\ -\hbar v|\vec{k}|e^{-i\theta(\vec{k})} & z - \sigma(z) \end{pmatrix}^{-1}$$

$$= \frac{1}{(z - \sigma(z))^2 - (\hbar v|\vec{k}|)^2}\begin{pmatrix} z - \sigma(z) & \hbar v|\vec{k}|e^{i\theta(\vec{k})} \\ \hbar v|\vec{k}|e^{-i\theta(\vec{k})} & z - \sigma(z) \end{pmatrix} \tag{24}$$

The eigenvalues are the poles of the Green's function. Therefore the energy $E(\vec{k})$ is given by

$$E - \sigma(E) = \pm\hbar v|\vec{k}| \tag{25}$$

For $|\vec{k}| = 0$ we have solution $E = E_0$ such that

$$E_0 - \sigma(E_0) = 0 \tag{26}$$

For small $\vec{k}$ we can write $E(\vec{k}) = E_0 + \delta E(\vec{k})$. Eventually we have a nice formula:

$$\delta E = \frac{\pm \hbar v |\vec{k}|}{1 - \sigma'(E_0)} \tag{27}$$

Finally the renormalized velocity v_r is

$$\frac{v_r}{v} = \frac{1}{1 + A/\theta^2} \tag{28}$$

where

$$A = \frac{6t^2}{4/3\,\pi^2 \gamma_0^2} \tag{29}$$

Therefore using a well established tight-binding model, we recover velocity renormalization consistent with that of[35]. In addition we find that this velocity renormalization is independent of the difference in potential of two planes.

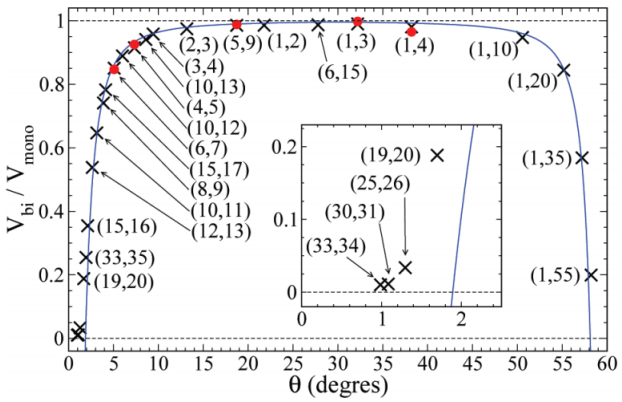

FIG. 2: Velocity ratio $v_b i/v_{\text{mono}}$ for a commensurate (n, m) bilayer cell versus rotation angle θ: circle, VASP; cross, TB calculations. The line is the model of Lopez dos Santos et al $v_b i/v_{\text{mono}} = 1 - 9[\tilde{t}/(v_{\text{mono}} K \sin(\theta/2))]$, with $\tilde{t} = 0.11$eV and $v_{\text{mono}} K = 2\sqrt{3}\gamma_0 \pi = 9.8$ eV . From[26]

As it is shown in Fig.2 a systematic study of the renormalization of the velocity close to the Dirac point is done[26], compared to its value in a monolayer graphene, for rotation angles θ varying between 0° and 60° (Fig.2). The renormalization of the velocity varies symmetrically around $\theta = 30^\circ$. Indeed, the two limit cases $\theta = 0^\circ$ (AA stacking) and $\theta = 60^\circ$ (AB stacking) are different, but Moiré patterns when $\theta \to 0^\circ$ and when $\theta \to 60^\circ$ are similar because a simple translation by a vector transforms an AA zone to an AB zone.

Focusing on angles smaller than 30°, it is defined[26] three regimes as a function of the rotation angle θ (Fig.2). For large $\theta (20^\circ \leq \theta \leq 30^\circ)$ the Fermi velocity is very close to that of graphene. For intermediate values of $\theta (3^\circ \leq \theta \leq 20^\circ)$ the perturbative theory of Lopez dos Santos et al. predicts correctly the velocity renormalization which is also in accordance to the above formula equation(28). For the small rotation angles ($\theta < 3^\circ$) a new regime occurs where the velocity tends to zero and perturbation theory can't be applied.

B. Electron lifetime

The two planes of the bilayer can have very different amount of disorder due to their different exposure to environment . For example the lower plane will be in contact with a substrate and the upper plane is exposed either to vacuum or to a gas (sensor application). Therefore it is of high interest to consider the limit case where defects are present in one plane and absent from the other plane. In the following we consider that defects are present only in the lower plane. If the two planes were decoupled, defects in one plane would affect electron lifetime in that plane but not in other one. Since the planes are coupled defects in one plane will also affect electronic lifetime in the other plane. In this chapter we discuss how such a repartition of defects impacts the electron lifetime. In chapter III based the present results we shall discuss how electron lifetime affects the overall electronic conduction of the bilayer.

If there is disorder in the lower plane the Bloch states of this plane will have a contribution to their self-energy which is imaginary. This can be represented in the simple possible model by a purey imaginary part of the potential evergy Δ

$$\Delta = -i\frac{\hbar}{\tau_-} \tag{30}$$

where τ_- is the lifetime in the lower plane due to disorder in the lower plane. Using formula 2.29 we see that electrons in the upper plane acquire an imaginary self-energy

$$\Im\sigma(z) = -\frac{i\hbar}{\tau_-} \times \frac{6t^2}{\gamma_0^2 4/3\pi^2\theta^2} = -\frac{i\hbar}{\tau_+} \tag{31}$$

Therefore the lifetimes τ_- and τ_+ in the lower and upper planes are related through:

$$\frac{\tau_+}{\tau_-} = \frac{\theta^2}{A} \tag{32}$$

where A is given by equation 29, and is same quantity as in the velocity renormalization expression eq.28.

IV. DENSITY OF STATES

We consider now the Density of States (DOS) on one plane as a function of position $\vec{r}$ in the Moiré structure. Here $\vec{r}$ will be position of the A and B atom.

$$\rho(E,\vec{r}) = \langle \vec{r}|\delta(E-H)|\vec{r'}\rangle \tag{33}$$

This quantity can be measured by STM and oscillations of the DOS are observed in experiments. To our knowledge a theory of this quantity didn't exist prior to this work and is presented now. According to the theory developed in Appendix B, the upper plane has an effective Hamiltonian which is modified by the coupling with lower plane. This effective Hamiltonian contains a self-energy discussed before which is independent of position and just renormalizes the velocity. It contains also a term that couples states with wave vector $\vec{k}$ and states with wave vector $\vec{k}+\vec{G}$ where $\vec{G}$ is a reciprocal vector of Moiré pattern. It is this coupling which mixes those states and will give oscillation of DOS with vector $\vec{G}$.

Due to our approximation on the inter-plane hopping $|t_i|$ only the 6 $\vec{G}_j$ with $|\vec{G}_j| = |\sqrt{3}K_d\theta|$ occur. These six G_j are along 6 directions with angles $\theta_j = 2\pi/6\, j$. After a long calculation(Appendix B) we get a compact formula for variation of the DOS[29]

$$\Rightarrow \frac{\Delta\rho(E,\vec{R},\varepsilon)}{\rho(E)} \cong \frac{2t^2}{(\hbar c K_d\theta)^2}\sum_{j=1}^{6}\cos(\vec{G}_j\cdot\vec{R}) \tag{34}$$

as we see this formula doesn't depend to type of atom ε (A or B atom), it oscillates with $\vec{G}$ as expected. Using $t \approx 0.12$eV we have

$$\Rightarrow \frac{\Delta\rho(E,\vec{R})}{\rho(E)} \cong \frac{1}{\theta_{deg}^2}\sum_{j=1}^{6} cos(\vec{G}_j\cdot\vec{R}) \tag{35}$$

where θ_{deg} is the rotation angle expressed in degrees. As it is clear the maximum value is obtained for $\vec{R}=0$ which is in the AA region and $\sum_{j=1}^{6} cos(\vec{G}_j\cdot\vec{R})$ is 6. For example for $\theta = 3^\circ$ the maximum value of relation variation of DOS is $\frac{6}{9}$ in the AA region which is strong. We note also that the relative variation rapidly decreases when θ increases.

We now compare our model results with those of tight-binding calculations. As shown in Fig.3 the overall agreement between tight-binding and model calculations is quite good. We observe in particular a reinforcement of the DOS in the AA region and a lowering in the AB regions. This behavior is a precursor of the electronic localization in AA region which is observed in the very low angle limit $\theta < 1-2^\circ$.

The main difference between the two approaches is the following. In the tight-binding results, two neighboring A and B atoms do not have the same DOS. In the analytical approach there is no such difference. As shown in Fig.4 average DOS of two neighboring A and B atoms is well reproduced by the analytical model. Yet the DOS on sub lattices A and B can differ by about $\pm 15\%$ as compared to averaged DOS. The reason of this discrepancy is not firmly established. It could be due to the use of perturbative theory. Another cause could be that we retained only one Fourier component of the transfer matrix element of $t(\vec{k})$. Indeed in the calculation by Castro Neto et. al[36] the authors retain also only one Fourier component of the transfer matrix $t(\vec{k})$, but do numerical non-perturbative calculation. They find also a DOS which is the same for neighboring A and B atoms.

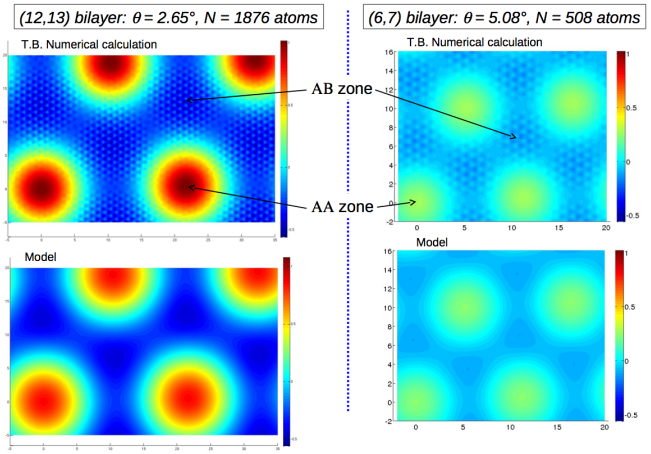

FIG. 3: Relative variation of the LDOS on top layer for two angles. Tight-binding results are in the top and corresponding analytical results are below.

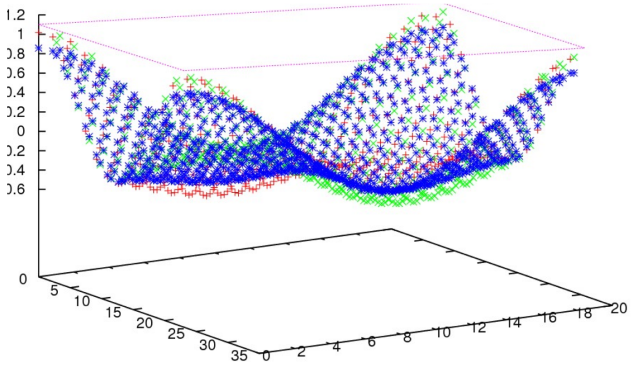

FIG. 4: 3D relative variation of DOS $\frac{\Delta\rho(E,\vec{R})}{\rho(E)}$. The green and red points correspond to A and B atoms with a difference of about $\pm 15\%$. Blue points corresponds to our analytical model which reproduce the average values of relative variation of DOSs on A and B atoms.

Conclusion

To conclude the present work we consider in particular the case of twisted bilayers of graphene. These systems have been discovered especially in graphene produced on Silicon Carbide and present original properties when compared with standard AB bilayers that occur for example in graphite. We analyze by perturbative theory and by numerical methods the density of states. We show that the electronic density of states presents periodic oscillations with the period of the geometric Moiré produced by these systems. We analyze also the role of defects on electron lifetime and in particular we consider the case where the defects are only in one layer.

* Electronic address: omid.faizy@nano.cnr.it
† Electronic address: guy.trambly@u-cergy.fr
‡ Electronic address: didier.mayou@grenoble.cnrs.fr

[1] S. Latil and L. Henrard, Phys. Rev. Lett. *97*, 036803 (2006).
[2] F.Zhang, B.Sahu, H.Min, A.H.MacDonald, Phys. Rev. B *82*, 035409 (2010)
[3] F. Varchon, P. Mallet, J.-Y. Veuillen, and L. Magaud, Phys. Rev. B *77*, 235412 (2008).
[4] T.Ohta, A.Bostwick, T.Seyller, K.Horn, E.Rotenberg Science *313*, 951 (2006)
[5] C.Coletti, C.Riedl, D.S.Lee, B.Krauss, L.Patthey, K.von Klitzing, J.H. Smet, U.Starke, Phys. Rev. *81*, 235401 (2010)
[6] I. Brihuega et al., Phys. Rev. Lett. *101*, 206802 (2008).
[7] J.Hass et al Appl. Phys. Lett *89*, 143106 (2006)
[8] J.Hass et al J.Phys: Condens. Matter *20*,323202(2008)
[9] K.V.Emtsev, F.Speck, Th. Seyller, L.Ley, J.D.Riley, Phys. Rev B *77*, 1553023 (2008)
[10] J. Hass, F. Varchon, J. E. Millan-Otoya, M. Sprinkle, N. Sharma, W. A. de Heer, C.Berger, P. N. First, L. Magaud, H. Conrad, Phys. Rev. Lett. *100*, 125504 (2008).
[11] M.Sprinkle et al Phys. Rev. Lett. *103*, 226803 (2009)
[12] J.Hicks et al Phys. Rev. B *83*, 205403 (2011)
[13] A.Luican, G.Li, A.Reina, J.Kong, R.R.Nair, K.S.Novoselov, A.K.Geim, E.Y.Andrei, Phys. Rev. Lett. *106*, 126802
[14] G.Li, A.Luican, L.M.B.Lopes dos Santos, A.H.Castro Neto, A.Reina, J.Kong, E.Y.Andrei, Nat. Phys. *6*, 109,(2010)
[15] D.L.Miller et al, Science *324*, 924 (2009)
[16] C. Berger et al., Science *312*, 1191 (2006).
[17] M.L.Sadowski, G.Martinez, M.Potemski, C.Berger, W.A.de Heer, Phys. Rev. Lett. *97*, 266405
[18] F.Varchon, P.Mallet, L.Magaud, J.-Y.Veuillen, Phys. Rev. B *77*, 165415 (2008) (2006)
[19] J. M. B. Lopez dos Santos, N. M. R. Peres, and A. H. Castro Neto, Phys. Rev. Lett. *99*, 256802 (2007) (2006)
[20] S.Latil, V.Meunier, L.Henrard, Phys. Rev. B *76*, 201402(R) (2008)
[21] S. Shallcross, S. Sharma, and O. A. Pankratov, Phys Rev.Lett. *101*, 056803 (2008)
[22] G.Mele
[23] E.Suarez Morell, J.D.Correa, P.Vargas, M.Pacheco, Z.Barticevic, Phys. Rev. B *82*, 121407 (R) (2010).
[24] R.Bistritzer and A.H. MacDonald, Proc. Natl. Acad. Sci. USA 108, 12233 (2011)
[25] R.Bistritzer and A.H.MacDonald, Phys. Rev. B *81*, 245412 (2010)
[26] G. Trambly de Laissardiere, D. Mayou, L. Magaud, Nano Let. 10, 804(2010)
[27] G.Trambly de Laissardiere
[28] J. M. Campanera, G. Savini, I. Suarez-Martinez, and M. I. Heggie Phys. Rev. B **75**, 235449 (2007).
[29] O. Faizy, G. Trambly de Laissardiere, D. Mayou.: to be submitted
[30] K. Sasaki, S. Murakami, and R. Saito; : Appl. Phys. Lett. 88, 113110 (2006)
[31] Yen-Hung Ho, Jhao-Ying Wu, Rong-Bin Chen, Yu-Huang Chiu, and Ming-Fa Lin Appl. Phys. Lett. **97**, 101905 (2010)
[32] Hongki Min.: *Graphene Nanoelectronics: Metrology, Synthesis, Properties and Applications*, NanoScience and Technology. Springer, 2012, p. 325
[33] Edward McCann.: *Graphene Nanoelectronics: Metrology, Synthesis, Properties and Applications*, NanoScience and Technology. Springer, 2012, p. 237
[34] I. Lobato and B. Partoens, PHYSICAL REVIEW B **83**, 165429 (2011)
[35] J. M. B. Lopes dos Santos, N. M. R. Peres, and A. H. Castro Neto, Phys Rev Lett, **99**, 256802 (2007)
[36] J. M. B. Lopes dos Santos, N. M. R. Peres, A. H. Castro Neto.: arXiv:1202.1088v1 [cond-mat.mtrl-sci]